Received: 25 September 2018 | Revised: 17 October 2018 | Accepted: 26 October 2018

DOI: 10.1111/cas.13853

ORIGINAL ARTICLE

WILEY Cancer Science

Involvement of dual-strand of the *miR-144* duplex and their targets in the pathogenesis of lung squamous cell carcinoma

Akifumi Uchida[1] | **Naohiko Seki**[2] | **Keiko Mizuno**[1] | **Shunsuke Misono**[1] | **Yasutaka Yamada**[2] | **Naoko Kikkawa**[2] | **Hiroki Sanada**[1] | **Tomohiro Kumamoto**[1] | **Takayuki Suetsugu**[1] | **Hiromasa Inoue**[1]

[1]Department of Pulmonary Medicine, Graduate School of Medical and Dental Sciences, Kagoshima University, Kagoshima, Japan

[2]Department of Functional Genomics, Graduate School of Medicine, Chiba University, Chiba, Japan

Correspondence
Naohiko Seki, Department of Functional Genomics, Chiba University Graduate School of Medicine, Chiba, Japan.
Email: naoseki@faculty.chiba-u.jp

Funding information
KAKENHI grants 18K09338, 17K09660, and 16K11224.

The prognosis of patients with advanced-stage lung squamous cell carcinoma (LUSQ) is poor, and effective treatment protocols are limited. Our continuous analyses of antitumor microRNAs (miRNAs) and their oncogenic targets have revealed novel oncogenic pathways in LUSQ. Analyses of our original miRNA expression signatures indicated that both strands of *miR-144* (*miR-144-5p*, the passenger strand; *miR-144-3p*, the guide strand) showed decreased expression in cancer tissues. Additionally, low expression of *miR-144-5p* significantly predicted a poor prognosis in patients with LUSQ by The Cancer Genome Atlas database analyses (overall survival, $P = 0.026$; disease-free survival, $P = 0.023$). Functional assays revealed that ectopic expression of *miR-144-5p* and *miR-144-3p* significantly blocked the malignant abilities of LUSQ cells, eg, cancer cell proliferation, migration, and invasion. In LUSQ cells, 13 and 15 genes were identified as possible oncogenic targets that might be regulated by *miR-144-5p* and *miR-144-3p*, respectively. Among these targets, we identified 3 genes (*SLC44A5*, *MARCKS*, and *NCS1*) that might be regulated by both strands of *miR-144*. Interestingly, high expression of *NCS1* predicted a significantly poorer prognosis in patients with LUSQ (overall survival, $P = 0.013$; disease-free survival, $P = 0.048$). By multivariate analysis, *NCS1* expression was found to be an independent prognostic factor for patients with LUSQ patients. Overexpression of NCS1 was detected in LUSQ clinical specimens, and its aberrant expression enhanced malignant transformation of LUSQ cells. Our approach, involving identification of antitumor miRNAs and their targets, will contribute to improving our understanding of the molecular pathogenesis of LUSQ.

KEYWORDS
lung squamous cell carcinoma, microRNA, *miR-144-3p*, *miR-144-5p*, *NCS1*

Abbreviations: Ago2, Argonaute2; D2R, dopamine D2 receptor; DFS, disease-free survival; GEO, Gene Expression Omnibus; LUAD, lung adenocarcinoma; LUSQ, lung squamous cell carcinoma; *MARCKS*, myristoylated alanine rich protein kinase C substrate; miRNA, microRNA; *NCS1*, neuronal calcium sensor 1; NSCLC, non-small cell lung cancer; OS, overall survival; qRT-PCR, real-time quantitative RT-PCR; RCC, renal cell carcinoma; RISC, RNA-induced silencing complex; siRNA, small interfering RNA; *SLC44A5*, solute carrier family 44 member 5; TCGA, The Cancer Genome Atlas.

1 | INTRODUCTION

Lung cancer is the leading cause of cancer-related deaths worldwide among both men and women.[1] Lung cancer includes 2 major clinicopathological categories: small cell lung cancer and NSCLC. The latter accounts for approximately 85% of all cases of lung cancer, and NSCLC tumors consist mainly of 3 subtypes: LUAD, LUSQ, and large cell carcinoma.[2] In patients with LUAD, currently developed treatment strategies (eg, epidermal growth factor receptor tyrosine kinase inhibitors, inhibitors of anaplastic lymphoma kinase, and immune checkpoint inhibitors) have dramatically improved OS rates in patients.[3-6] In contrast, in patients with LUSQ, the lack of early diagnostic tools and effective treatment protocols has resulted in a poor OS rate in patients with LUSQ.[7,8] Therefore, identification of therapeutic target molecules is essential for achieving improved outcomes in patients with LUSQ.

MicroRNAs are a class of small, noncoding RNAs (19-22 nt in length). These molecules regulate gene expression by repressing translation or cleaving RNA transcripts in a sequence-dependent manner.[9] Interestingly, a single miRNA species could regulate a vast number of protein-coding and noncoding RNA transcripts.[10] In human disease cells, aberrantly expressed miRNAs trigger the failure of orderly and controlled RNA networks.[11] Numerous studies have shown that aberrant expression of miRNAs and dysregulated RNA networks are deeply involved in human diseases, including cancer.[12-16]

Through our continuing work, we have identified antitumor miRNAs and their target oncogenic genes in LUSQ.[17-22] Moreover, detailed analyses of our original miRNA expression signatures by RNA sequencing have revealed that passenger strands of miRNAs actually act as antitumor miRNAs and are involved in cancer pathogenesis.[23-25] Additionally, our recent studies showed that both strands of the *miR-144* duplex (ie, the passenger strand *miR-144-5p* and the guide strand *miR-144-3p*) are downregulated in bladder cancer and RCC tissues and act as antitumor miRNAs.[26,27] The involvement of both strands of the miRNA duplex in cancer pathogenesis is a new concept for cancer research.

Several cohort analyses by TCGA database have indicated that low expression of *miR-144-5p* predicts poor prognosis in patients with LUSQ (OS, $P = 0.026$; DFS, $P = 0.023$). Thus, both strands of the *miR-144* duplex are involved in LUSQ molecular pathogenesis. Here, we aimed to verify that *miR-144-5p* and *miR-144-3p* possess antitumor functions. We also sought to identify their molecular targets, thereby revealing new details of LUSQ pathogenesis.

2 | MATERIALS AND METHODS

2.1 | Clinical specimen collection, cell lines, and cell culture

The present study was approved by the Bioethics Committee of Kagoshima University Hospital (Kagoshima, Japan) (approval nos 26-164). Written prior informed consent and approval were obtained from all patients. In total, 30 LUSQ specimens and 20 noncancerous lung specimens were collected from patients who underwent thoracic surgery at Kagoshima University Hospital from 2010 to 2013. The pathological stages of LUSQ were classified according to the International Association for the Study of Lung Cancer TNM classification, 7th edition.[28] The clinicopathological features of the patients are shown in Table 1. The procedure for RNA extraction from formalin-fixed, paraffin-embedded specimens was described in previous studies.[19]

In addition, we evaluated 2 LUSQ cell lines (EBC-1 and SK-MES-1), obtained from the Japanese Cancer Research Resources Bank (Osaka, Japan) and ATCC (Manassas, VA, USA), respectively. Cell culture, extraction of total RNA, and extraction of protein were carried out as described in our earlier reports.[18,19,21]

2.2 | Quantitative real-time RT-PCR

The procedure for qRT-PCR has been described previously.[18,22,29] The expression levels of miRNAs were analyzed by TaqMan qRT-PCR assays (assay IDs 002148 and 002676; Applied Biosystems, Foster City, CA, USA). Data were normalized to the expression of *RNU48* (assay ID 001006; Applied Biosystems). *NCS1* expression levels were determined using TaqMan probes and primers (assay ID Hs00179522_m1; Applied Biosystems), and *GAPDH* (assay ID Hs99999905_m1; Applied Biosystems) was used for normalization.

TABLE 1 Characteristics of lung cancer and noncancerous cases

A. Characteristics of lung cancer cases	**n (%)**
Total number	30
Median age, years (range)	71 (50-88)
Sex	
Male	29 (96.7)
Female	1 (3.3)
Pathological stage	
IA	5 (16.7)
IB	9 (30.0)
IIA	2 (6.7)
IIB	6 (20.0)
IIIA	7 (23.3)
IIIB	1 (3.3)
B. Characteristics of noncancerous cases	**n**
Total number	20
Median age, years (range)	70.5 (50-88)
Sex	
Male	20
Female	0

Pathological stage of lung cancer was classified according to the International Association for the Study of Lung Cancer TNM classification, 7th edition.[28]

TABLE 2 Characteristics and immunohistochemical status of patients included in tissue microarray analysis

A. Immunohistochemical status and characteristics of cases with lung squamous cell carcinoma

Patient no.	Grade	T	N	M	Pathological stage	Immunohistochemical staining intensity
23	2	2	1	0	IIB	(+)
24	2	2	0	0	IB	(+++)
25	2	1	0	0	IA	(+++)
26	1	2	1	0	IIB	(+)
27	2	1	0	0	IA	(++)
28	1	3	0	0	IIB	(++)
29	1	2	0	0	IB	(+++)
30	2	2	0	0	IB	(+++)
31	3	2	0	0	IB	(+++)
32	3	2	1	0	IIB	(+)
33	3	2	0	0	IB	(+)
34	3	2	1	0	IIB	(+++)
35	2	3	1	0	IIIA	(++)
36	3	2	1	0	IIA	(+++)
37	3	3	0	0	IIB	(++)
38	3	2	0	0	IB	(++)
39	3	2	1	0	IIB	(+++)
40	3	2	0	0	IB	(++)
41	2-3	3	0	0	IIB	(+++)
42	3	1	2	0	IIIA	(+)
43	3	2	0	0	IB	(+)
44	3	2	0	0	IB	(+)

B. Immunohistochemical status of noncancerous cases

Patient no.	Immunohistochemical staining intensity
69	(+)
70	(−)
71	(−)
72	(+)
73	(+)
74	(+)
75	(+)
76	(++)
77	(+)
78	(+)
79	(+)
80	(+)

Pathological stages of lung cancer were classified according to the International Association for the Study of Lung Cancer TNM classification.[28]

2.3 | Transfection of LUSQ cells with mature miRNA and siRNA

The following mature miRNA species were used in this study: mirVana miRNA mimic, hsa-*miR-144-5p* (product ID MC12631; Applied Biosystems), hsa-*miR-144-3p* (product ID MC11051; Applied Biosystems), and negative control miRNA, anti-miR negative control #1 (catalog no. AM17010; Applied Biosystems). The following siRNAs were used: Stealth Select RNAi siRNA, si-*NCS1* (P/N HSS118732 and HSS118734; Invitrogen, Carlsbad, CA, USA), and negative control miRNA/siRNA, anti-miR negative control #1 (catalog no. AM17010; Applied Biosystems). The transfection procedures were described previously.[18,20,22]

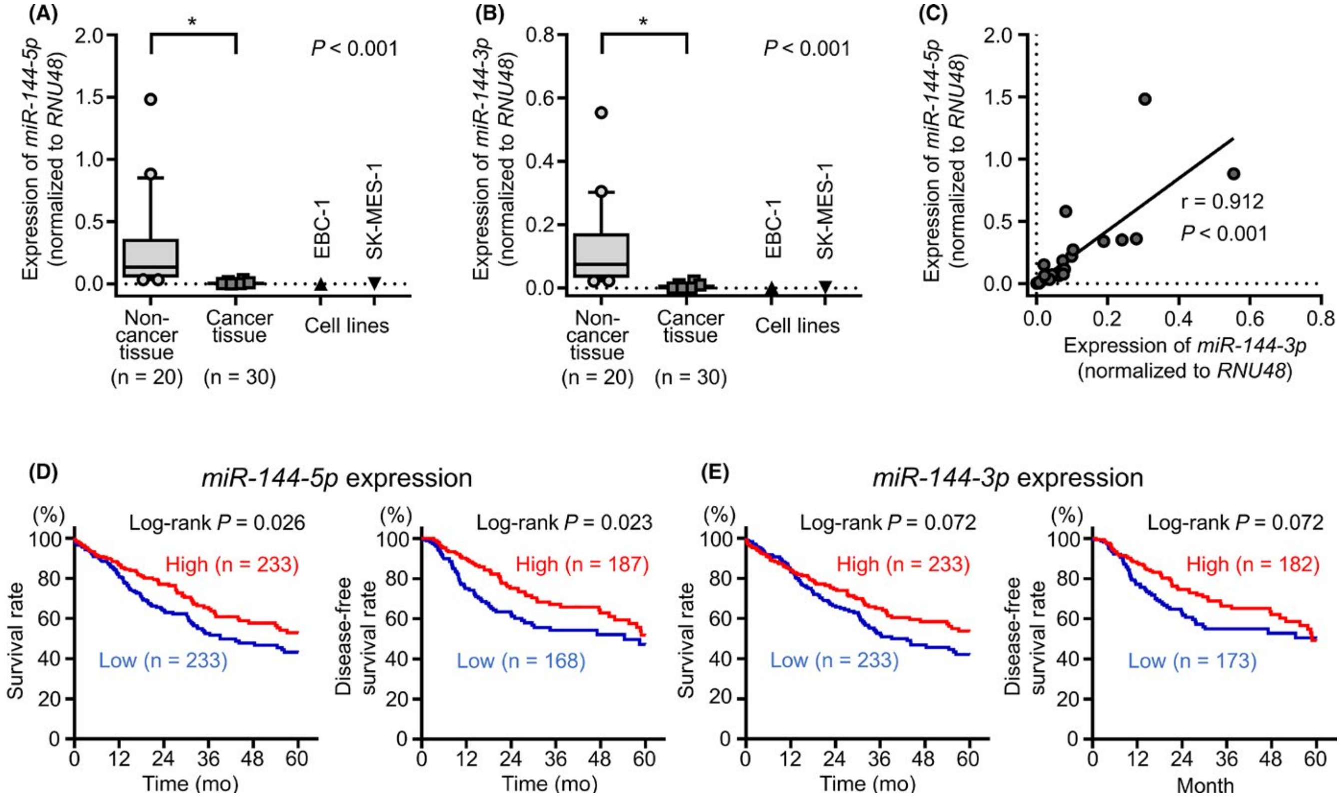

FIGURE 1 Expression levels of *miR-144-5p* and *miR-144-3p* in clinical lung squamous cell carcinoma (LUSQ) specimens and cell lines, and analysis of the expression levels of *miR-144-5p and miR-144-3p* in patients with LUSQ using The Cancer Genome Atlas (TCGA) database. A, Expression levels of *miR-144-5p* in clinical specimens and cell lines (EBC-1 and SK-MES-1). B, Expression levels of *miR-144-3p* in clinical specimens and cell lines (EBC-1 and SK-MES-1). Data were normalized to *RNU48*. **P* < 0.001. C, Correlation between the expression levels of *miR-144-5p* and *miR-144-3p* in clinical specimens. Expression of *miR-144-5p* and *miR-144-3p* in clinical specimens showed a positive correlation (r = 0.912, P < 0.001). D, Kaplan-Meier curve of 5-year overall survival and 5-year disease-free survival according to *miR-144-5p* expression among patients with LUSQ in TCGA database (P = 0.026 and P = 0.023, respectively). E, Kaplan-Meier curve of 5-year overall survival and 5-y disease-free survival according to *miR-144-3p* expression in patients with LUSQ in TCGA database (P = 0.072 and P = 0.072, respectively)

2.4 | Incorporation of *miR-144-5p* and *miR-144-3p* into RISC: Assessment by Ago2 immunoprecipitation

MicroRNAs were transfected into EBC-1 cells by reverse transfection. After a 48-hour incubation period, miRNAs were isolated by immunoprecipitation using a microRNA Isolation Kit for Human Ago2 (Wako, Osaka, Japan). We then assessed the expression of Ago2-conjugated miRNAs by qRT-PCR, as described in previous studies.[30,31]

2.5 | Cell proliferation, migration, and invasion assays

Protocols for determining cell proliferation, migration, and invasion were described previously.[17,22]

2.6 | Identification of putative target genes regulated by *miR-144-5p* and *miR-144-3p* in LUSQ cells

Gene expression analyses by oligo microarray and in silico analyses were used to identify putative target genes regulated by *miR-144-5p* and *miR-144-3p*. The microarray data were deposited in the GEO repository under accession number GSE115801. Putative target genes having binding sites for *miR-144-5p* and *miR-144-3p* were detected by TargetScanHuman version 7.2 (http://www.targetscan.org/vert_72/). The GEO database (GSE19188) was used for assessment of the association between target genes and expression of NSCLC clinical specimens. Identification of *miR-144-5p* and *miR-144-3p* target genes was carried out as described in Figure S1.

2.7 | Clinical database analysis

The clinical significance of miRNAs and their target genes in LUSQ was investigated with TCGA database (https://tcga-data.nci.nih.gov/tcga/). The gene expression and clinical data were retrieved from cBioPortal (http://www.cbioportal.org/) and OncoLnc (http://www.oncolnc.org) (data downloaded on April 28, 2018).[31-33]

2.8 | Plasmid construction and dual-luciferase reporter assay

Wild-type or deletion-type sequences targeted by *miR-144-5p* and *miR-144-3p* were inserted into the psiCHECK-2 vector (C8021; Promega, Madison, WI, USA).

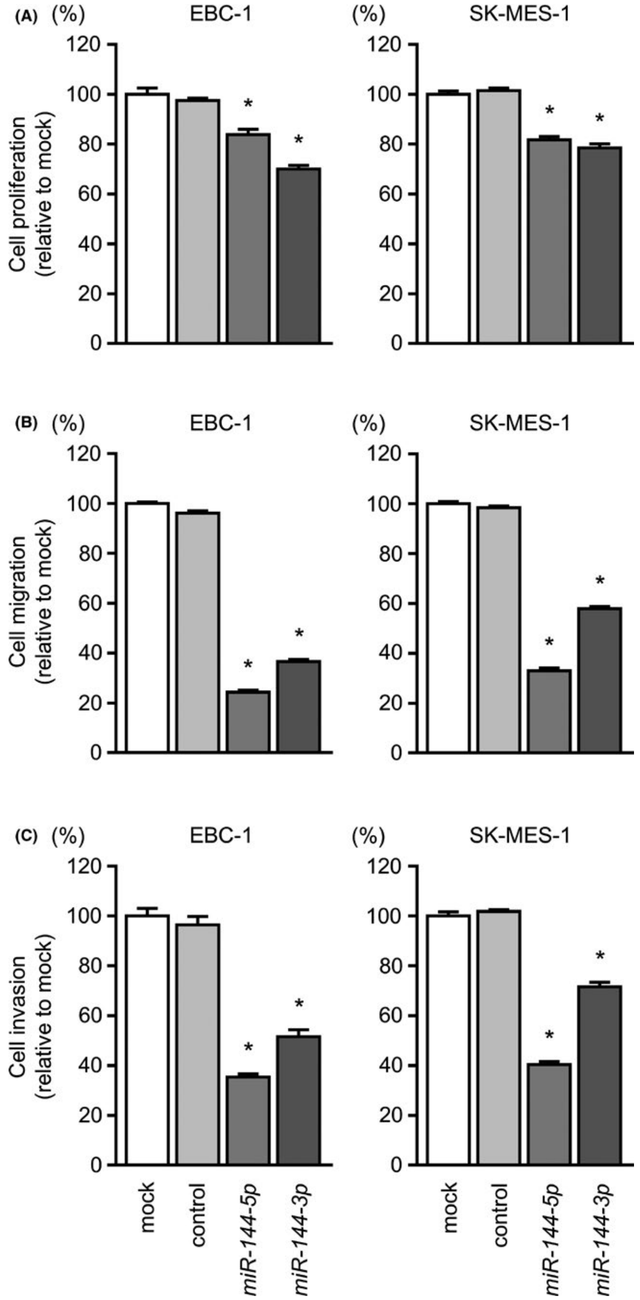

FIGURE 2 Functional assays of *miR-144-5p* and *miR-144-3p* in lung squamous cell carcinoma cell lines. A, Cell proliferation was determined by XTT assays 72 hours after transfection with *miR-144-5p* and *miR-144-3p*. B, Cell migration was measured by wound healing assays. C, Cell invasion was determined by Matrigel invasion assays. Cell proliferation, migration, and invasion were significantly suppressed in *miR-144-5p* and *miR-144-3p* transfectants compared with those in mock and control transfectants. *$P < 0.001$

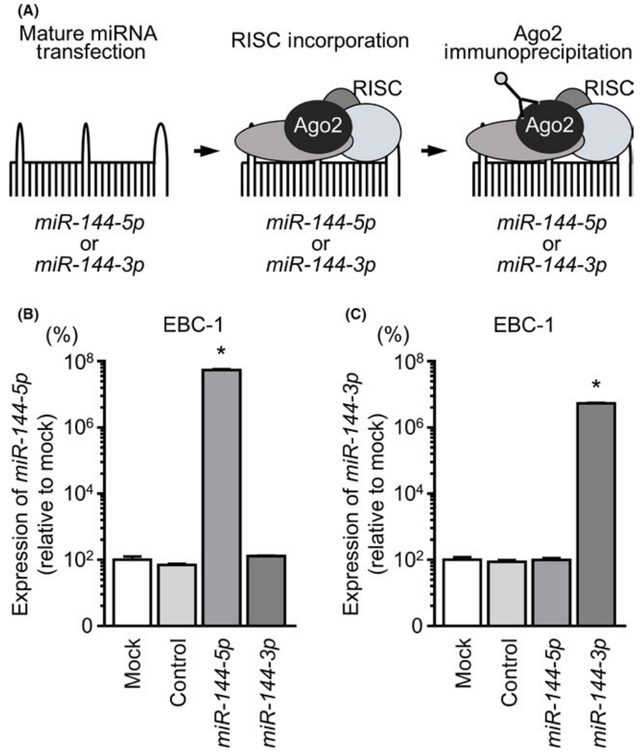

FIGURE 3 Incorporation of *miR-144-5p* and *miR-144-3p* into the RNA-induced silencing complex (RISC) in lung squamous cell carcinoma cell lines. A, Schematic diagram of isolation of RISC-incorporated microRNAs by Argonaute2 (Ago2) immunoprecipitation. In LUSQ cells, if *miR-144-5p* or *miR-144-3p* regulated gene activities, *miR-144-5p* or *miR-144-3p* was incorporated into the RISC. By carrying out immunoprecipitation with Ago2, which has a central role in the RISC, *miR-144-5p* or *miR-144-3p* incorporated into the RISC was detected. B, Expression levels of *miR-144-5p* following immunoprecipitation by Ago2. C, Expression levels of *miR-144-3p* following immunoprecipitation by Ago2. *$P < 0.001$

After cotransfecting miRNA and the constructed vector into EBC-1 and SK-MES-1 cells, firefly and *Renilla* luciferase activities were measured using a dual Luciferase assay kit (Promega). The procedure was described previously.[18,20,22]

2.9 | Western blot analysis and immunohistochemistry

The procedures for western blotting and immunohistochemistry were described previously.[21,22] Membranes were immunoblotted with monoclonal anti-NCS1 Abs (1:1000 dilution; ab129166; Abcam, Cambridge, UK) and monoclonal anti-GAPDH Abs (1:20 000 dilution; MAB374; EMD Millipore, Billerica, MA, USA).

Immunohistochemistry was carried out with a VECTASTAIN Universal Elite ABC Kit (catalog no. PK-6200; Vector Laboratories, Burlingame, CA, USA) according to the manufacturer's protocol. Primary rabbit mAbs against NCS1 (ab129166; Abcam) were used at a 1:100 dilution at 4°C overnight. The characteristics of patients included in the tissue microarray are described in Table 2. The procedure for immunohistochemistry was described previously.[18,22,34]

TABLE 3 Common putative target genes regulated by *miR-144-5p* and *miR-144-3p* in lung squamous cell carcinoma cells

Entrez gene ID	Gene symbol	Description	SK-MES-1 *miR-144-5p* transfectant Log_2 ratio	SK-MES-1 *miR-144-3p* transfectant Log_2 ratio	GSE19188 Log fold-change	TCGA database 5-y OS *P* value
23413	*NCS1*	Neuronal calcium sensor 1	−1.04	−1.04	1.31	0.013
204962	*SLC44A5*	Solute carrier family 44 member 5	−1.28	−1.96	3.07	0.325
4082	*MARCKS*	Myristoylated alanine rich protein kinase C substrate	−1.53	−1.04	1.44	0.872

Lower and upper percentiles of The Cancer Genome Atlas (TCGA) database were both 50.
GSE, Gene Expression Omnibus dataset results; OS, overall survival.

2.10 | Statistical analysis

All data were analyzed using SPSS version 23 software (IBM SPSS, Chicago, IL, USA). Differences between 2 groups were analyzed by Mann-Whitney *U* tests, and those between multiple groups were examined by one-way ANOVA and Tukey tests for post-hoc analysis. Differences between survival rates were analyzed by Kaplan-Meier survival curves and log-rank statistics. Univariate and multivariate analyses for OS using TCGA database were carried out by Cox proportional hazards regression analyses.

3 | RESULTS

3.1 | Downregulation of *miR-144-5p* and *miR-144-3p* in LUSQ clinical specimens and their clinical significance

The expression levels of *miR-144-5p* and *miR-144-3p* were markedly decreased in LUSQ tissues in comparison with those in noncancerous tissues ($P < 0.001$; Figure 1A,B). Positive correlations between the expression of *miR-144-5p* and *miR-144-3p* were confirmed by Spearman's rank tests ($r = 0.912$ and $P < 0.001$; Figure 1C). In 2 cancer cell lines, EBC-1 and SK-MES-1, the expression levels of *miR-144-5p* and *miR-144-3p* were extremely low (Figure 1A,B).

By analyses using TCGA database, low expression of *miR-144-5p* significantly predicted poor prognosis compared with high expression of *miR-144-5p* (5-year OS, $P = 0.026$; 5-year DFS, $P = 0.023$; Figure 1D). Low expression of *miR-144-3p* also tended to predict poor prognosis compared with high expression of *miR-144-3p* in LUSQ patients (5-year OS, $P = 0.072$; 5-year DFS, $P = 0.072$; Figure 1E).

3.2 | Ectopic expression of *miR-144-5p* and *miR-144-3p* suppressed cancer cell proliferation, migration, and invasion in LUSQ cells

To verify the functional roles of *miR-144-5p* and *miR-144-3p* in LUSQ, EBC-1 and SK-MES-1 cells were transfected with mature *miR-144-5p* and *miR-144-3p* sequences. Cell proliferation assays showed significant inhibition of cell growth in *miR-144-5p* and *miR-144-3p* transfectants (Figure 2A). Moreover, cell migration and Matrigel invasion were significantly inhibited by *miR-144-5p* or *miR-144-3p* transfection (Figures 2B,C). In migration and invasion analyses, *miR-144-5p* had stronger antitumor effects than *miR-144-3p*.

3.3 | Incorporation of *miR-144-5p* and *miR-144-3p* into RISC in LUSQ cells

To verify whether the *miR-144-5p* passenger strand could be incorporated into the RISC in LUSQ cells, we undertook immunoprecipitation for Ago2, which is essential for formation of the RISC, in cells transfected with either *miR-144-5p* or *miR-144-3p*. Isolated Ago2-bound miRNAs were analyzed by qRT-PCR to examine the interactions between *miR-144-5p* or *miR-144-3p* and Ago2. A conceptual diagram of this analysis is shown in Figure 3A.

In EBC-1 cells, *miR-144-5p* transfectants showed higher expression levels of *miR-144-5p* than did mock transfectants or miR-control or *miR-144-3p* ($P < 0.001$) transfectants (Figure 3B). Similarly, after *miR-144-3p* transfection, we detected *miR-144-3p* using Ago2 immunoprecipitation ($P < 0.001$; Figure 3C).

3.4 | Identification of putative target genes regulated by *miR-144-5p* and *miR-144-3p* in LUSQ cells

Next, we aimed to identify *miR-144-5p* and *miR-144-3p* target genes. To this end, we undertook a combination of in silico and genome-wide gene expression analyses, as shown in Figure S1. Using TargetScanHuman database analysis, 1785 and 3776 putative target genes were found to have binding sites for *miR-144-5p* and *miR-144-3p*, respectively. Among these genes, we selected genes that were upregulated in NSCLC clinical expression profiles from the GEO database (accession no. GSE19188). Next, we merged gene expression analysis data using *miR-144-5p-* or *miR-144-3p*-transfected SK-MES-1 cells (GEO accession no. GSE115801). This analysis yielded *miR-144-5p-* and *miR-144-3p*-controlled genes (n = 13 and 15, respectively) in LUSQ cells (Table S1 and S2).

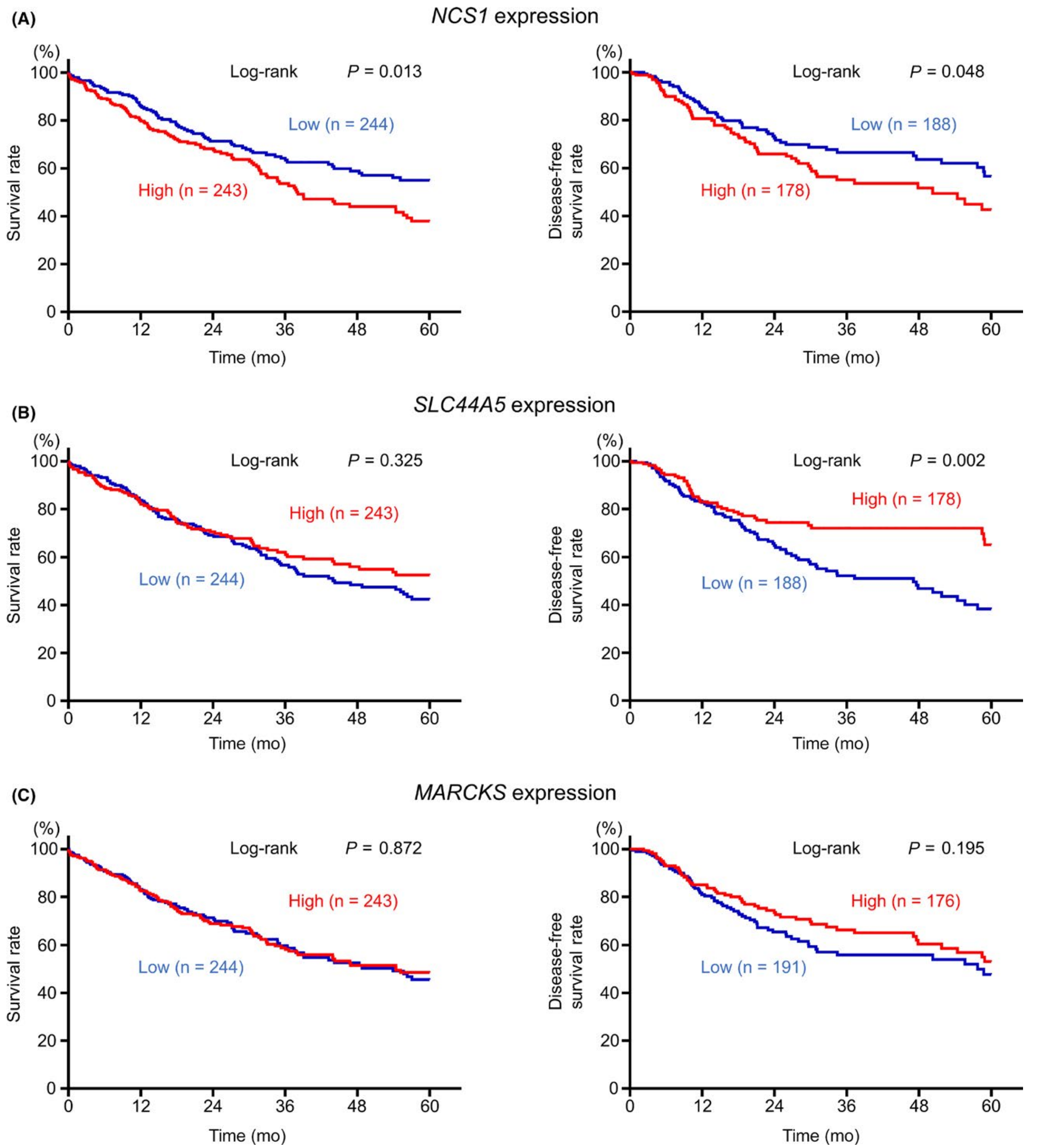

FIGURE 4 A, Kaplan-Meier curve of 5-year overall survival (OS) and 5-year disease-free survival (DFS) according to *NCS1* expression among patients with lung squamous cell carcinoma (LUSQ) in The Cancer Genome Atlas (TCGA) database. The prognosis and DFS of patients with LUSQ with high expression of *NCS1* was significantly worse than those with low expression ($P = 0.013$ and $P = 0.048$, respectively). B, Kaplan-Meier curve of 5-year OS and 5-year DFS according to *SLC44A5* expression among patients with LUSQ in TCGA database. There were no significant differences between the prognosis of patients with LUSQ according to *SLC44A5* expression ($P = 0.325$). Conversely, DFS in patients with LUSQ was significantly higher in the high expression group than in the low expression group ($P = 0.002$). C, Kaplan-Meier curve of 5-year OS and 5-year DFS according to *MARCKS* expression among patients with LUSQ in TCGA database. There were no significant differences in prognosis or DFS in patients with LUSQ according to *MARCKS* expression ($P = 0.872$ and $P = 0.195$, respectively)

Overall, 3 putative target genes (*NCS1*, *SLC44A5*, and *MARCKS*) were coordinately regulated by both *miR-144-5p* and *miR-144-3p* (Table 3). The TCGA database analysis showed that high *NCS1* expression significantly predicted a poor prognosis in patients with LUSQ (5-year OS, $P = 0.013$; 5-year DFS, $P = 0.048$; Figure 4A). Subsequently, we focused on *NCS1* and validated the functional significance of LUSQ cells.

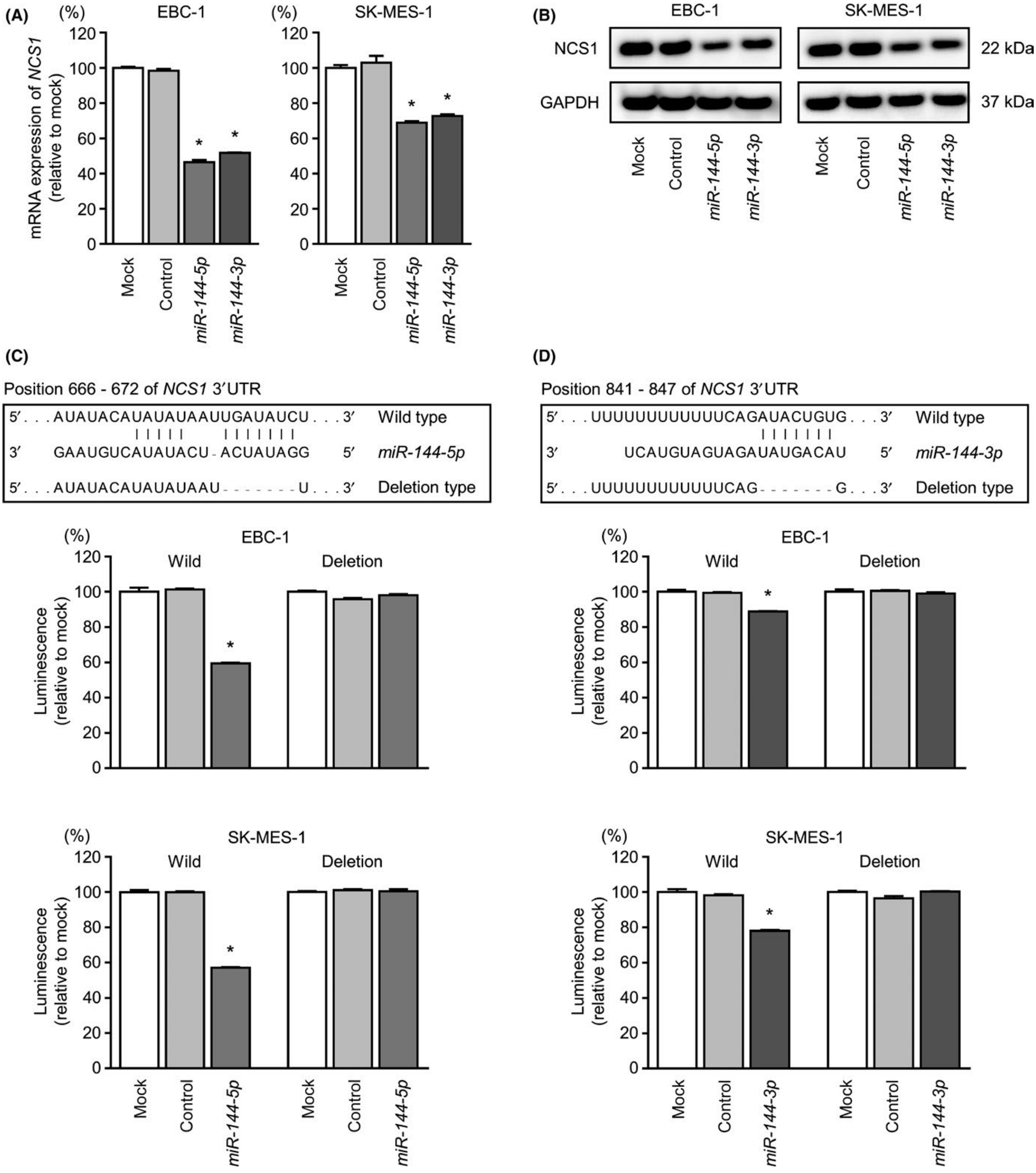

FIGURE 5 Direct regulation of *NCS1* by *miR-144-5p* and *miR-144-3p* in lung squamous cell carcinoma cell lines. A, Expression levels of *NCS1* mRNA 72 hours after transfection with *miR-144-5p* and *miR-144-3p* using *GAPDH* as an internal control. B, NCS1 protein expression by western blot analysis 72 hours after transfection with *miR-144-5p* and *miR-144-3p* in EBC-1 and SK-MES-1 cell lines. GAPDH was used as a loading control. C, Putative *miR-144-5p* binding sites in the 3′-UTR of *NCS1* mRNA. Dual luciferase reporter assays using vectors encoding putative *miR-144-5p* target sites in the *NCS1* 3′-UTR (position 666-672) for both wild-type and deleted regions. Normalized data were calculated as *Renilla*/firefly luciferase activity ratios. D, Putative *miR-144-3p* binding sites in the 3′-UTR of *NCS1* mRNA. Dual luciferase reporter assays using vectors encoding putative *miR-144-3p* target sites in the *NCS1* 3′-UTR (position 841-847) for both wild-type and deleted regions. Normalized data were calculated as *Renilla*/firefly luciferase activity ratios. $^{*}P < 0.001$

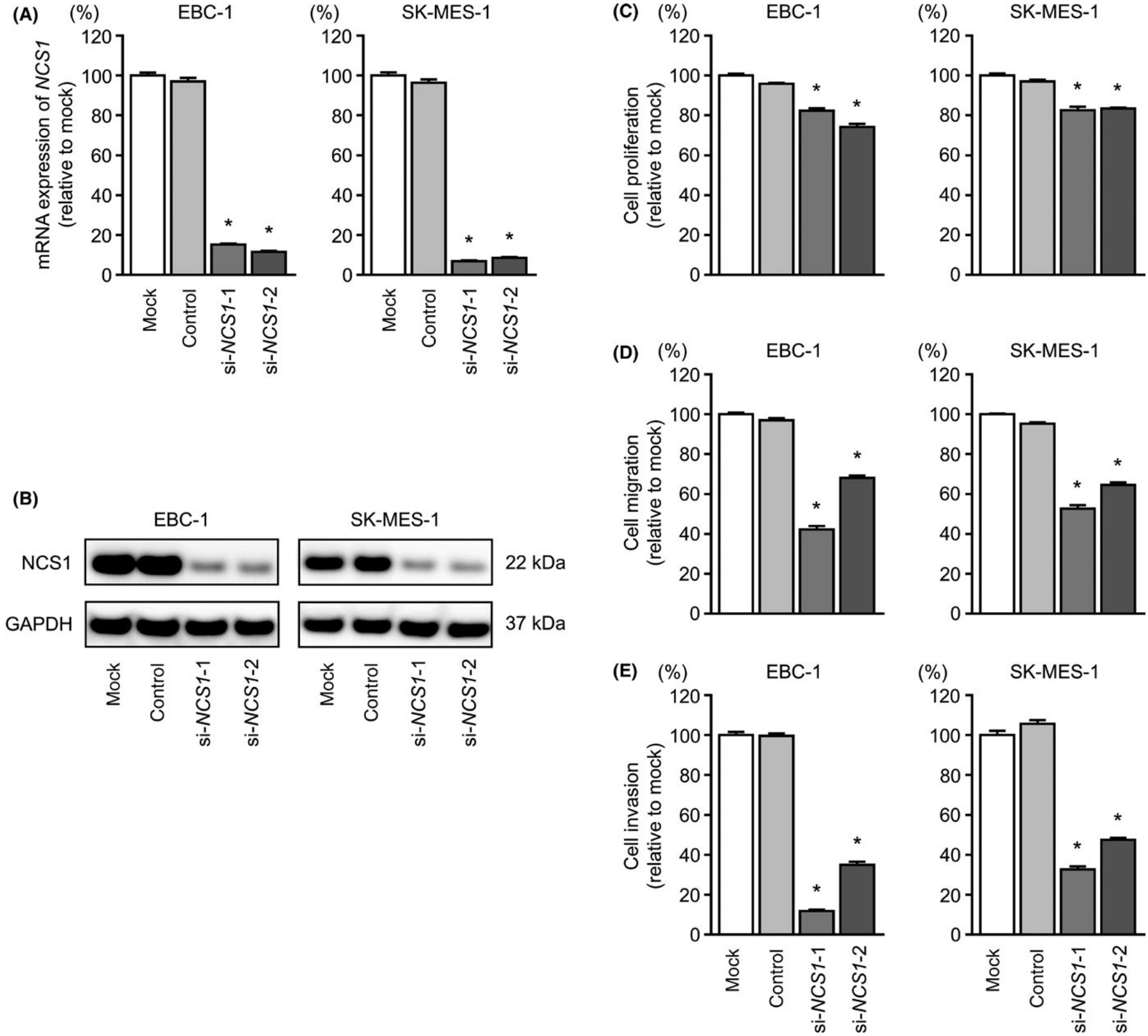

FIGURE 6 Effects of *NCS1* silencing in lung squamous cell carcinoma cell lines. A, mRNA expression of *NCS1* 72 hours after transfection with si-*NCS1* using *GAPDH* as an internal control. B, NCS1 protein expression by western blot analysis 72 hours after transfection with si-*NCS1*-1 and si-*NCS1*-2 in EBC-1 and SK-MES-1 cell lines. GAPDH was used as a loading control. C, Cell proliferation was identified by XTT assays 72 hours after transfection with si-*NCS1*-1 and si-*NCS1*-2. D, Cell migration was measured by wound healing assays. E, Cell invasion was determined by Matrigel invasion assays. *$P < 0.001$

3.5 | Direct regulation of *NCS1* by *miR-144-5p* and *miR-144-3p* in LUSQ cells

We then examined whether *NCS1* mRNA and NCS1 protein expression were suppressed by restoration of *miR-144-5p* and *miR-144-3p* in LUSQ cells. *NCS1* mRNA and NCS1 protein levels were significantly decreased by *miR-144-5p* or *miR-144-3p* transfection compared with those in mock- or miR-control-transfected cells (Figure 5A,B).

Next, we carried out luciferase reporter assays in EBC-1 and SK-MES-1 cells to validate the direct binding of *miR-144-5p* and *miR-144-3p* to *NCS1* mRNA. The TargetScanHuman database projected the existence of binding sites in the 3′- UTR of *NCS1* (*miR-144-5p*, position 666-672; *miR-144-3p*, position 841-847; Figure 5C,D). Accordingly, we undertook luciferase reporter assays with vectors that contained either the wild-type or deletion-type 3′-UTR of *NCS1*. Our results showed that the luminescence intensities were markedly reduced by transfection with *miR-144-5p* or *miR-144-3p* and the vector harboring the wild-type 3′-UTR of *NCS1*. In contrast, transfection with the deletion-type vector did not reduce the luminescence intensities in EBC-1 or SK-MES-1 cells (Figure 5C,D). These findings indicated that both strands of the *miR-144* duplex bound directly to the 3′-UTR of *NCS1*.

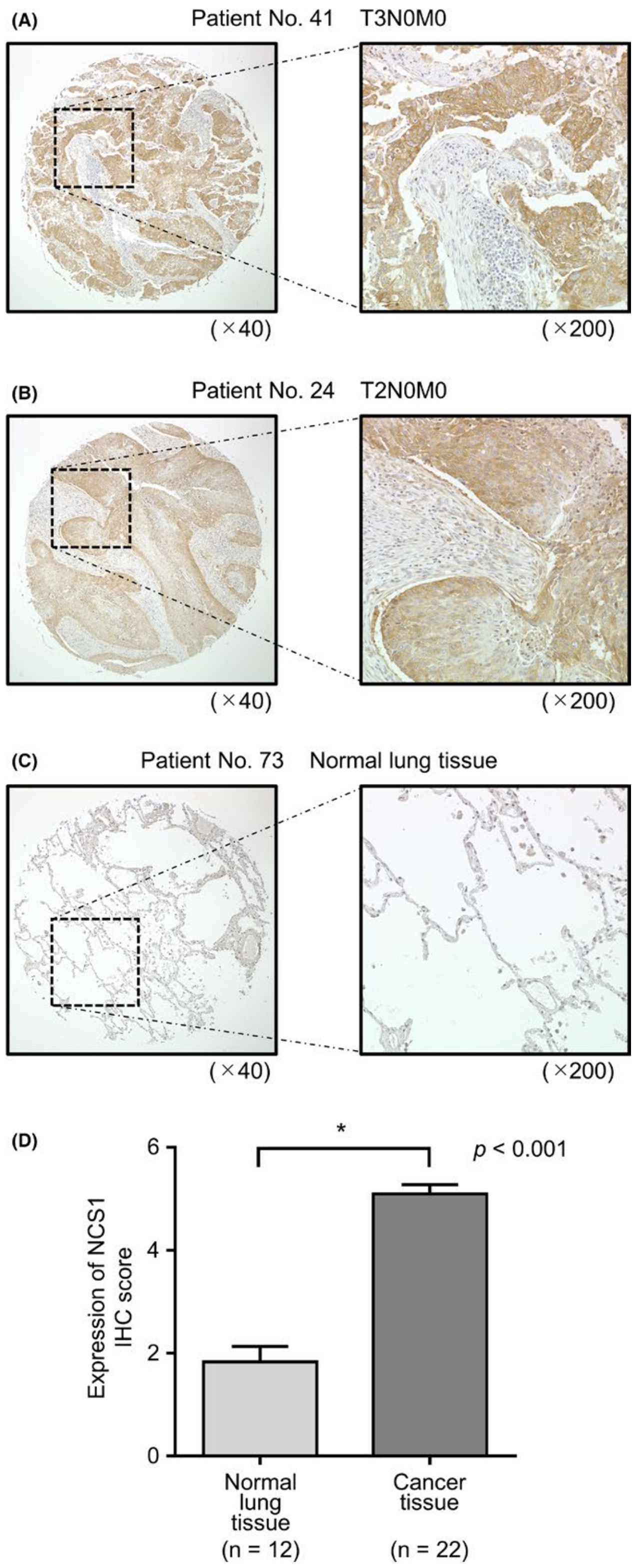

FIGURE 7 Expression of neuronal calcium sensor 1 (NCS1) in clinical lung squamous cell carcinoma (LUSQ) tissue. A-C, Immunohistochemistry staining of NCS1 in LUSQ specimens and normal lung tissue using a tissue microarray. Overexpression of NCS1 was observed in the cytoplasm of cancer cells, whereas negative or low expression of NCS1 was observed in normal cells. D, Comparison of the scoring of NCS1 expression in clinical lung specimens. NCS1 expression in LUSQ tissue was significantly higher than in normal lung tissue. *$P < 0.001$

3.6 | *NCS1* knockdown inhibited cell proliferation, migration, and invasion in LUSQ cells

We examined the effects of *NCS1* knockdown in EBC-1 and SK-MES-1 cells using 2 types of si-*NCS1* oligos: si-*NCS1*-1 and si-*NCS1*-2. Both siRNAs effectively downregulated *NCS1* mRNA and NCS1 protein expression (Figure 6A,B).

Cancer cell proliferation, migration, and invasive abilities were markedly inhibited by si-*NCS1* transfection compared with those in mock or control EBC-1 and SK-MES-1 cells (Figure 6C-E).

3.7 | Expression of NCS1 in LUSQ clinical specimens and its clinical significance

Immunohistochemical analyses of LUSQ clinical specimens indicated that NCS1 protein was strongly expressed in LUSQ cells, but showed infrequent and weak expression in normal lung cells (Table 2 and Figure 7).

Finally, univariate and multivariate Cox hazard regression analyses were used to evaluate the clinical significance of *NCS1* expression for OS in patients with LUSQ. Multivariate analysis showed that *NCS1* expression was an independent predictive factor for OS (hazard ratio = 1.508, $P = 0.007$; Figure 8).

4 | DISCUSSION

In our previous studies, we showed that both strands of the *miR-145* duplex (the guide strand *miR-145-5p* and the passenger strand *miR-145-3p*) were significantly downregulated in cancer tissues. These miRNAs were also found to have antitumor functions, and their targets were involved in NSCLC pathogenesis.[20,35] Thus, research focusing on both strands of the miRNA duplex is important for improving outcomes in cancer.

In this study, we found that both *miR-144-5p* and *miR-144-3p* had tumor-suppressing effects in LUSQ cells and controlled several oncogenes. In an analysis of previous studies of the functional significance of the *miR-144* duplex, the antitumor function of *miR-144-3p* was reported in several type of cancers.[36-41] For example, expression of *miR-144-3p* suppressed cancer cell proliferation in glioblastoma and hepatocellular carcinoma through targeting *c-MET* and *SGK3*, respectively.[36,37] In laryngeal squamous cell carcinoma, *miR-144-3p* inhibited the cancer cell epithelial-mesenchymal transition phenotype through targeting *ETS-1*.[38] These data indicated that *miR-144-3p* was a pivotal tumor suppressor, and that downregulation of *miR-144-3p* enhanced cancer cell aggressiveness. Recent studies reported that some long noncoding RNAs (metastasis-associated lung adenocarcinoma transcript 1 [*MALAT1*] and taurine upregulated 1 [*TUG1*]) acted as competing endogenous RNAs and that their overexpression attenuated the expression of *miR-144-3p* in cancer cells.[39,40] Another study showed that interleukin-1β affected *miR-144-3p* at the transcriptional level and that interleukin-1β levels were significantly higher in patients with LUAD and LUSQ.[41]

(A)

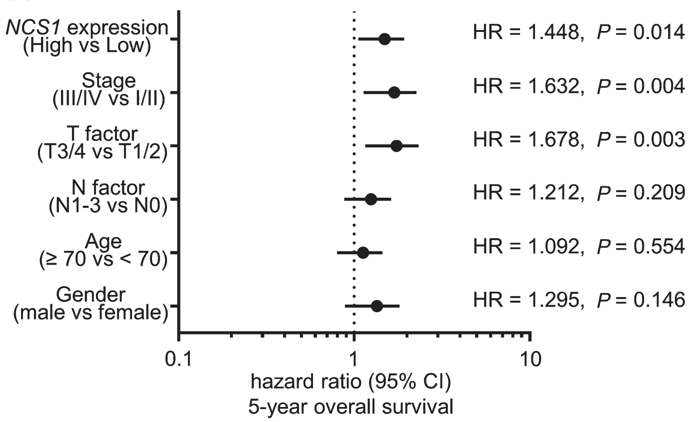

(B)

Multivariate cox proportional hazards regression analysis

	hazard ratio	95% CI	*p*-value
NCS1	1.508	1.118 – 2.032	0.007
Stage	1.425	0.948 – 2.142	0.088
T factor	1.446	0.961 – 2.176	0.077

FIGURE 8 Analysis of the expression levels of *NCS1* in patients with lung squamous cell carcinoma using The Cancer Genome Atlas (TCGA) database. A, Forest plot of univariate Cox proportional hazards regression analysis of 5-year overall survival using TCGA database. B, Multivariate Cox proportional hazards regression analysis of 5-year overall survival using TCGA database. CI, confidence interval; HR, hazard ratio

In contrast to *miR-144-3p* analyses, few reports have examined the functional significance of *miR-144-5p* in cancer cells. Analyses of miRNA signatures by RNA sequencing showed that both strands of *miR-144-5p* and *miR-144-3p* were frequently downregulated in several cancers.[26,27] In our studies, we focused on both strands of the *miR-144* duplex and investigated the antitumor functions and targets of the duplex in cancer cells.[26,27] Our previous studies showed that both strands of the *miR-144* duplex had antitumor functions in bladder cancer and RCC and that both miRNAs coordinately targeted *CCNE1*/*CCNE2* and *SDC3*, respectively.[26,27] This study is the third paper reporting the antitumor functions of both strands of the *miR-144* duplex in cancer cells. Importantly, low expression of *miR-144-5p* and *miR-144-3p* significantly predicted short survival in patients with RCC.[27] Moreover, high expression of the oncogenic genes controlled by these miRNAs also predicted short survival in patients with RCC, suggesting that the *miR-144* duplex and its targets were deeply involved in RCC pathogenesis.[27]

In this study, 3 genes (*NCS1*, *SLC44A5*, and *MARCKS*) were found to be coordinately controlled by both *miR-144-5p* and *miR-144-3p* in LUSQ cells. *MARCKS* is a major substrate of protein kinase C.[42] Recent studies have shown that *MARCKS* plays a pivotal role in cancer development and progression.[42] Moreover, in lung cancer, aberrant *MARCKS* expression was detected in clinical specimens, and *MARCKS* expression was implicated in this disease.[43,44]

Among the 3 targets, we focused on *NCS1* because its aberrant expression significantly predicted poor prognosis in patients. The NCS1 protein is a member of the NCS family, which harbors a functional Ca^{2+} binding domain and *N*-terminally myristoylated site.[45,46] Previous studies have reported that NCS1 is a multifunctional protein involved in exocytosis, neurite outgrowth, neuroprotection, axonal regeneration, and nuclear Ca^{2+} regulation.[45,46] Furthermore, NCS1 interacts with various proteins to control their functions.[45,46] For example, NCS1 interacts with D2R and inhibits D2R-mediated signaling pathways.[47] Interestingly, activation of D2R-mediated signaling suppresses lung cancer aggressiveness.[48] Moreover, aberrant expression of *NCS1* could interfere with D2R-mediated signaling and might be involved in LUSQ cell progression.

Our functional assays showed that inhibition of *NCS1* by siRNA suppressed cancer cell migration and invasion in LUSQ cells. Moreover, in multivariate Cox proportional hazards regression analysis, expression of *NCS1* predicted poor prognosis in patients with LUSQ. Another study showed that overexpression of *NCS1* promoted cell invasion and migration in breast cancer cells and that *NCS1* overexpression was associated with poor prognosis in these patients.[49] These findings indicate that aberrantly expressed *NCS1* is involved in cancer cell aggressiveness. Thus, *NCS1* could be a novel diagnostic and therapeutic target for patients with LUSQ.

In conclusion, genes coordinately controlled by the *miR-144* duplex (*miR-144-5p* and *miR-144-3p*) were found to be related to LUSQ pathogenesis. Our findings describing the involvement of the passenger strand *miR-144-5p* are the first report of this phenomenon in LUSQ pathogenesis. *NCS1* expression was directly regulated by the *miR-144* duplex in LUSQ cells. Aberrantly expressed *NCS1* enhanced LUSQ cell aggressiveness. Thus, elucidation of antitumor miRNAs controlling RNA networks could provide novel prognostic markers and therapeutic targets for this disease.

ACKNOWLEDGMENTS

This study was supported by KAKENHI grants 18K09338, 17K09660, and 16K11224.

CONFLICT OF INTEREST

The authors declare no conflicts of interest.

ORCID

Akifumi Uchida http://orcid.org/0000-0001-8038-6377
Yasutaka Yamada http://orcid.org/0000-0002-0070-1590

REFERENCES

1. Fitzmaurice C, Allen C, Barber RM, et al. Global, regional, and national cancer incidence, mortality, years of life lost, years lived with disability, and disability-adjusted life-years for 32 cancer groups, 1990 to 2015: a systematic analysis for the global burden of disease study. *JAMA Oncol*. 2017;3:524-548.
2. Travis WD. Pathology of lung cancer. *Clin Chest Med*. 2011;32:669-692.
3. Zhou C, Wu YL, Chen G, et al. Final overall survival results from a randomised, phase III study of erlotinib versus chemotherapy as first-line treatment of EGFR mutation-positive advanced non-small-cell lung cancer (OPTIMAL, CTONG-0802). *Ann Oncol*. 2015;26:1877-1883.
4. Soria JC, Ohe Y, Vansteenkiste J, et al. Osimertinib in untreated EGFR-mutated advanced non-small-cell lung cancer. *N Engl J Med*. 2018;378:113-125.
5. Peters S, Camidge DR, Shaw AT, et al. Alectinib versus Crizotinib in untreated ALK-positive non-small-cell lung cancer. *N Engl J Med*. 2017;377:829-838.
6. Reck M, Rodriguez-Abreu D, Robinson AG, et al. Pembrolizumab versus chemotherapy for PD-L1-positive non-small-cell lung cancer. *N Engl J Med*. 2016;375:1823-1833.
7. Sandler AB, Schiller JH, Gray R, et al. Retrospective evaluation of the clinical and radiographic risk factors associated with severe pulmonary hemorrhage in first-line advanced, unresectable non-small-cell lung cancer treated with Carboplatin and Paclitaxel plus bevacizumab. *J Clin Oncol*. 2009;27:1405-1412.
8. Paz-Ares L, Tan EH, O'Byrne K, et al. Afatinib versus gefitinib in patients with EGFR mutation-positive advanced non-small-cell lung cancer: overall survival data from the phase IIb LUX-Lung 7 trial. *Ann Oncol*. 2017;28:270-277.
9. Bartel DP. MicroRNAs: genomics, biogenesis, mechanism, and function. *Cell*. 2004;116:281-297.
10. Bartel DP. MicroRNAs: target recognition and regulatory functions. *Cell*. 2009;136:215-233.
11. Gulyaeva LF, Kushlinskiy NE. Regulatory mechanisms of microRNA expression. *J Transl Med*. 2016;14:143.
12. Lin S, Gregory RI. MicroRNA biogenesis pathways in cancer. *Nat Rev Cancer*. 2015;15:321.
13. Baer C, Claus R, Plass C. Genome-wide epigenetic regulation of miRNAs in cancer. *Cancer Res*. 2013;73:473-477.
14. Koshizuka K, Hanazawa T, Arai T, Okato A, Kikkawa N, Seki N. Involvement of aberrantly expressed microRNAs in the pathogenesis of head and neck squamous cell carcinoma. *Cancer Metastasis Rev*. 2017;36:525-545.
15. Mizuno K, Mataki H, Seki N, Kumamoto T, Kamikawaji K, Inoue H. MicroRNAs in non-small cell lung cancer and idiopathic pulmonary fibrosis. *J Hum Genet*. 2017;62:57-65.
16. Koshizuka K, Hanazawa T, Fukumoto I, Kikkawa N, Okamoto Y, Seki N. The microRNA signatures: aberrantly expressed microRNAs in head and neck squamous cell carcinoma. *J Hum Genet*. 2017;62:3-13.
17. Mataki H, Enokida H, Chiyomaru T, et al. Downregulation of the microRNA-1/133a cluster enhances cancer cell migration and invasion in lung-squamous cell carcinoma via regulation of Coronin1C. *J Hum Genet*. 2015;60:53-61.
18. Mataki H, Seki N, Chiyomaru T, et al. Tumor-suppressive microRNA-206 as a dual inhibitor of MET and EGFR oncogenic signaling in lung squamous cell carcinoma. *Int J Oncol*. 2015;46:1039-1050.
19. Mizuno K, Seki N, Mataki H, et al. Tumor-suppressive microRNA-29 family inhibits cancer cell migration and invasion directly targeting LOXL2 in lung squamous cell carcinoma. *Int J Oncol*. 2016;48:450-460.
20. Mataki H, Seki N, Mizuno K, et al. Dual-strand tumor-suppressor microRNA-145 (miR-145-5p and miR-145-3p) coordinately targeted MTDH in lung squamous cell carcinoma. *Oncotarget*. 2016;7:72084-72098.
21. Kumamoto T, Seki N, Mataki H, et al. Regulation of TPD52 by antitumor microRNA-218 suppresses cancer cell migration and invasion in lung squamous cell carcinoma. *Int J Oncol*. 2016;49:1870-1880.
22. Suetsugu T, Koshizuka K, Seki N, et al. Downregulation of matrix metalloproteinase 14 by the antitumor miRNA, miR-150-5p, inhibits the aggressiveness of lung squamous cell carcinoma cells. *Int J Oncol*. 2018;52:913-924.
23. Yonemori K, Seki N, Idichi T, et al. The microRNA expression signature of pancreatic ductal adenocarcinoma by RNA sequencing: anti-tumour functions of the microRNA-216 cluster. *Oncotarget*. 2017;8:70097-70115.
24. Koshizuka K, Nohata N, Hanazawa T, et al. Deep sequencing-based microRNA expression signatures in head and neck squamous cell carcinoma: dual strands of pre-miR-150 as antitumor miRNAs. *Oncotarget*. 2017;8:30288-30304.
25. Goto Y, Kurozumi A, Arai T, et al. Impact of novel miR-145-3p regulatory networks on survival in patients with castration-resistant prostate cancer. *Br J Cancer*. 2017;117:409-420.
26. Matsushita R, Seki N, Chiyomaru T, et al. Tumour-suppressive microRNA-144-5p directly targets CCNE1/2 as potential prognostic markers in bladder cancer. *Br J Cancer*. 2015;113:282-289.
27. Yamada Y, Arai T, Kojima S, et al. Regulation of antitumor miR-144-5p targets oncogenes: direct regulation of syndecan-3 and its clinical significance. *Cancer Sci*. 2018;109:2919-2936.
28. Mirsadraee S, Oswal D, Alizadeh Y, Caulo A, van Beek E Jr. The 7th lung cancer TNM classification and staging system: review of the changes and implications. *World J Radiol*. 2012; 4: 128-134.
29. Mizuno K, Mataki H, Arai T, et al. The microRNA expression signature of small cell lung cancer: tumor suppressors of miR-27a-5p and miR-34b-3p and their targeted oncogenes. *J Hum Genet*. 2017;62:671-678.
30. Yamada Y, Koshizuka K, Hanazawa T, et al. Passenger strand of miR-145-3p acts as a tumor-suppressor by targeting MYO1B in head and neck squamous cell carcinoma. *Int J Oncol*. 2018;52:166-178.
31. Koshizuka K, Hanazawa T, Kikkawa N, et al. Regulation of ITGA3 by the anti-tumor miR-199 family inhibits cancer cell migration and invasion in head and neck cancer. *Cancer Sci*. 2017;108:1681-1692.
32. Gao J, Aksoy BA, Dogrusoz U, et al. Integrative analysis of complex cancer genomics and clinical profiles using the cBioPortal. *Science Signal*. 2013; 6: pl1.
33. Arai T, Okato A, Kojima S, et al. Regulation of spindle and kinetochore-associated protein 1 by antitumor miR-10a-5p in renal cell carcinoma. *Cancer Sci*. 2017;108:2088-2101.
34. Kojima S, Chiyomaru T, Kawakami K, et al. Tumour suppressors miR-1 and miR-133a target the oncogenic function of purine nucleoside phosphorylase (PNP) in prostate cancer. *Br J Cancer*. 2012;106:405-413.
35. Misono S, Seki N, Mizuno K, et al. Dual strands of the miR-145 duplex (miR-145-5p and miR-145-3p) regulate oncogenes in lung adenocarcinoma pathogenesis. *J Hum Genet*. 2018;63:1015-1028.
36. Lan F, Yu H, Hu M, Xia T, Yue X. miR-144-3p exerts anti-tumor effects in glioblastoma by targeting c-Met. *J Neurochem*. 2015;135:274-286.

37. Wu M, Huang C, Huang X, Liang R, Feng Y, Luo X. MicroRNA-144-3p suppresses tumor growth and angiogenesis by targeting SGK3 in hepatocellular carcinoma. *Oncol Rep*. 2017;38:2173-2181.
38. Zhang SY, Lu ZM, Lin YF, et al. miR-144-3p, a tumor suppressive microRNA targeting ETS-1 in laryngeal squamous cell carcinoma. *Oncotarget*. 2016;7:11637-11650.
39. Wang Y, Zhang Y, Yang T, et al. Long non-coding RNA MALAT1 for promoting metastasis and proliferation by acting as a ceRNA of miR-144-3p in osteosarcoma cells. *Oncotarget*. 2017;8:59417-59434.
40. Cao J, Han X, Qi X, Jin X, Li X. TUG1 promotes osteosarcoma tumorigenesis by upregulating EZH2 expression via miR-144-3p. *Int J Oncol*. 2017;51:1115-1123.
41. Wu C, Xu B, Zhou Y, et al. Correlation between serum IL-1beta and miR-144-3p as well as their prognostic values in LUAD and LUSC patients. *Oncotarget*. 2016;7:85876-85887.
42. Fong LWR, Yang DC, Chen CH. Myristoylated alanine-rich C kinase substrate (MARCKS): a multirole signaling protein in cancers. *Cancer Metastasis Rev*. 2017;36:737-747.
43. Reddy SP, Natarajan V, Dudek AZ. MARCKS is marked in combating lung cancer growth and acquired resistance. *Am J Respir Crit Care Med*. 2014;190:1084-1086.
44. Chen CH, Statt S, Chiu CL, et al. Targeting myristoylated alanine-rich C kinase substrate phosphorylation site domain in lung cancer. Mechanisms and therapeutic implications. *Am J Respir Crit Care Med*. 2014; 190: 1127-1138.
45. Burgoyne RD, Haynes LP. Sense and specificity in neuronal calcium signalling. *Biochim Biophys Acta*. 2015;1853:1921-1932.
46. Boeckel GR, Ehrlich BE. NCS-1 is a regulator of calcium signaling in health and disease. *Biochim Biophys Acta*. 2018;1865:1660-1667.
47. Kabbani N, Negyessy L, Lin R, Goldman-Rakic P, Levenson R. Interaction with neuronal calcium sensor NCS-1 mediates desensitization of the D2 dopamine receptor. *J Neurosci*. 2002;22:8476-8486.
48. Hoeppner LH, Wang Y, Sharma A, et al. Dopamine D2 receptor agonists inhibit lung cancer progression by reducing angiogenesis and tumor infiltrating myeloid derived suppressor cells. *Mol Oncol*. 2015;9:270-281.
49. Moore LM, England A, Ehrlich BE, Rimm DL. Calcium sensor, NCS-1, promotes tumor aggressiveness and predicts patient survival. *Mol Cancer Res*. 2017;15:942-952.

SUPPORTING INFORMATION

Additional supporting information may be found online in the Supporting Information section at the end of the article.

How to cite this article: Uchida A, Seki N, Mizuno K, et al. Involvement of dual-strand of the *miR-144* duplex and their targets in the pathogenesis of lung squamous cell carcinoma. *Cancer Sci*. 2019;110:420–432. https://doi.org/10.1111/cas.13853